Supplementary Information

Ru/CeO_2 Catalysts for Supercritical Water Gasification of Glycerol: Stability, Activity, and Coke Hydrothermal Oxidation

Tomasz Kondratowicz,[a†] Aurélien Quenet,[a,b†] Xujun Li,[a] Andrea Testino,[a,c] Oliver Kröcher,[a,b] Frédéric Vogel[a,d] and David Baudouin[a*]

[a] *Paul Scherrer Institute (PSI), Center for Energy and Environmental Sciences, CH-5232 Villigen PSI, Switzerland*

[b] *Institute of Chemical Sciences and Engineering, École Polytechnique Fédérale de Lausanne, (EPFL), 1015 Lausanne, Switzerland*

[c] *Institute of Materials, École Polytechnique Fédérale de Lausanne, (EPFL), 1015 Lausanne, Switzerland*

[d] *University of Applied Sciences Northwestern Switzerland (FHNW), School of Engineering and Environment, 5210 Windisch, Switzerland*

[†]These authors contributed equally to the research and are to be considered co first authors.

*Corresponding author: david.baudouin@psi.ch

Contents

Experimental section

Catalyst preparation

Synthesis of Ru/CeO_2 catalysts

Commercial CeO_2 pellets (Z-3254) from Daiichi Kigenso Kagaku Kogyo Co., Ltd, Japan, were ground in an agate mortar and sieved to the desired grain size (0.5-0.8 mm). Then, the sample was calcined at different temperatures (500, 700 and 900°C) for 4 h under Ar flow (100 $mL \cdot min^{-1} \cdot g^{-1}$) applying a heating rate of $5°C \cdot min^{-1}$. The uncalcined sample was designated as CeO_2, while the calcined one was denoted as CeO_2_x, where *x* expresses the temperature of calcination.

Two CeO_2 samples calcined at 700 and 900°C were selected as supports and then modified by incipient wetness impregnation (IWI) technique with aqueous solutions of $RuNO(NO_3)_3$ (31.3 % Ru, Alfa Aesar). The concentration of the solution was adjusted to achieve the desired catalyst loadings after thermal treatment, assuming no losses during the impregnation step and complete filling of the support pores. In a recent paper,[1] an optimal ruthenium surface loading was identified for Ru nanoparticles supported on carbon nanofibers, which was found to be in the 0.4-0.7 $atom_{Ru,sfc} \cdot nm^{-2}$ range. In this study, a value of 0.5 $atom_{Ru,sfc} \cdot nm^{-2}$ was used as target to prepare various Ru/CeO_2 catalysts using ceria supports calcined at different temperatures. Since the total pore volume of CeO_2_900 was minor (0.022 $cm^3 \cdot g^{-1}$), only 0.11 wt.% Ru was introduced onto the surface of this sample, while higher loadings of 0.25, 0.44 and 1.00 wt.% Ru were deposited on CeO_2_700, as this support sample exhibited higher porosity (0.068 $cm^3 \cdot g^{-1}$). The impregnated samples were dried in a vertical oven in a quartz reactor (i.d. = 45 mm, L = 600 mm, with a sintered disc in the middle to support the sample) at 120°C for 10 h (heating rate of $5°C \cdot min^{-1}$) under Ar flow (100 $mL \cdot min^{-1} \cdot g^{-1}$), followed by reduction at 300°C for 4 h (heating rate $5°C \cdot min^{-1}$) in H_2/N_2 (5:95 v/v, 150 $mL \cdot min^{-1}$). After the reactor was cooled down to room temperature, the catalysts were passivated for 24 h by allowing air to diffuse through the pierced tubular reactor to ensure slow exposure to air. This procedure allowed the formation of a thin RuO_2 oxide layer on the Ru^0 particle surface in a controlled manner, which would be easily reduced under reactive conditions. The Ru-loaded samples were designated as *y*%Ru/CeO_2_x, where *y* is the nominal Ru content.

Synthesis of Ru/CNF catalyst

The commercially available carbon nanofibers (NC7000, Nanocyl) were first crushed and sieved to the desired grain size (0.5-0.8 mm). The CNFs were then purified in 1 M KOH (reflux 2 h, 125°C), after which the particles were filtered, thoroughly washed with distilled water (until the filtrate became neutral), dried at 110°C overnight and sieved again to the fraction of interest (0.5–0.8 mm). Afterwards, the CNF particles were modified in a similar way as the CeO_2 samples, with the difference that a Ru solution was used, which allowed the introduction of 5.00 wt.% Ru onto the CNF surface. This sample was designated as 5.00%Ru/CNF and was the reference catalyst in this study.

Characterization

Crystallographic structures of samples were determined with a Bruker Advance D8 diffractometer with $CuK\alpha_1$ radiation (λ = 1.5406 Å) operated at 40 kV and 30 mA. Solid samples were mounted on PMMA sample holders, and XRD patterns were recorded in the range of 2θ = 10-90° with a step of 0.02°. Before the measurements, the CeO_2 pellets were ground in an agate mortar to form a powder, while the samples with a fraction of 0.5-0.8 mm were used without grinding. Coherence length (as estimation of CeO_2 crystallite size) was evaluated via Rietveld refinement and GSAS-II software.[2]

Nitrogen adsorption-desorption isotherms were recorded at -196°C using an Autosorb iQ-XR (Quantachrome) instrument. Before the measurements, samples were degassed for 3.5 h under vacuum at 350°C. Total pore volumes (V_{total}) were obtained from amounts of nitrogen adsorbed at a relative pressure of $p/p_0 \approx 0.99$, while the specific surface areas (S_{BET}) were determined by the BET method.

High-resolution TEM images taken with a probe-corrected JEOL JEM-ARM200F (NeoARM) microscope equipped with a Gatan OneView camera, LaB6 cathode, cold field emission gun (Cold FEG) working at an accelerating voltage of 60 kV. Samples for the TEM observations were prepared by drop-casting on film-free lacey carbon grids (Ted Pella Inc.) using ethanol or dimethylformamide (DMF) to disperse the ground CeO_2- and CNF-based catalysts, respectively. Note that the very poor contrast between $Ru^0@RuO_2$ (core@shell) and CeO_2 using TEM or STEM-HAADF modes, makes the evaluation of Ru particle size distribution unrealistic by electron microscopy. Indeed, EDX analysis is necessary to confirm the

composition of the observed nanoparticles; however, obtaining statistically meaningful data (ideally from >400 particles) requires an impractically high effort (see Results and Discussion section for details).

Inductively coupled plasma optical emission spectroscopy (ICP-OES) analyses were carried out to determine the Ru concentration in the liquid samples (process water, PW) collected during the SCWG experiment. Measurements were performed on an Agilent 5100 ICP-OES. Calibration was performed by construction of a standard curve using ICP standards from Sigma-Aldrich.

Thermogravimetric analyses (TGA) were performed using a TGA/DSC 1 Star system (Mettler Toledo), coupled to a Themo mass spectrometer (Pfeiffer Vacuum). Approximately 50 mg of sample was loaded in an Al_2O_3 crucible and first heated up in air to 110°C for 30 min at a heating rate of 5°C·min^{-1} to get rid of the moisture. Subsequently, the temperature was increased up to 1000°C with a ramp of 5°C·min^{-1}. Analyses were performed with air as reactive and Ar as protective gas (at a flow rate of 50 mL·min^{-1} each). The evolved gases analysis (EGA) was performed via mass spectrometry, where the main mass lines of C (m/z = 12), H_2O (m/z = 18), N_2 (m/z = 28), O_2 (m/z = 32), and CO_2 (m/z = 44) were analysed.

Catalytic tests

Continuous SCWG setup and analytics

The catalytic performance was investigated on a flow SCWG system called Konti-I (a piping and instrumentation diagram, P&ID, is shown in Fig. S0). The plug-flow fixed-bed reactor was a stainless steel (316L grade) tube from SITEC-Sieber Engineering AG (L = 460 mm, o.d. = 14.3 mm, i.d. = 8 mm,). The catalyst bed was located in the centre of the reactor, hold in place by three sizes of stainless steel wire mesh (0.08, 0.25 and 0.50 mm) on top of a hollow stainless steel rod. The remaining reactor volume was filled with inert α-Al_2O_3 beads (diameter 1.5 mm, porosity 0.03 cm^3·g^{-1}, Alfa Aesar) to improve the flow distribution and minimize the risk of dead zones. After connecting the reactor, a high-pressure pump (Knauer 80 P) supplied DI water, and then the system was pressurised to 275 bar by a backpressure regulator (BPR, Tescom) and heated up (400°C) by a series of three electrical heaters. Subsequently, the water tank was replaced with an aqueous glycerol solution (3-10 wt.%), and the catalyst bed temperature was adjusted to the desired values (400-430°C). The nitrogen line was opened

to dilute the gas effluent and limit GC detector peak saturation for H_2, as well as to increase the gas pressure for low gas production experiments. After the reactor outlet, the heat exchanger was located to cool down the effluent. The effluent entered a phase separator from which the liquid and gaseous phases left the plant. Gas measurements were taken every 15 min to determine the amount of gas produced and its composition. In turn, liquid samples were collected every 1 h to monitor the carbon content in the process water. After the test was completed, the reactor was slowly cooled overnight in a DI water flow. The pressure was then released, and the catalyst bed was dried in an inert gas flow. The catalyst bed was then separated from the Al_2O_3 beads using sieves and optionally tweezers. The samples after the catalytic test were marked as y%Ru/CeO_2_x_*S*, where *S* denotes the spent catalyst.

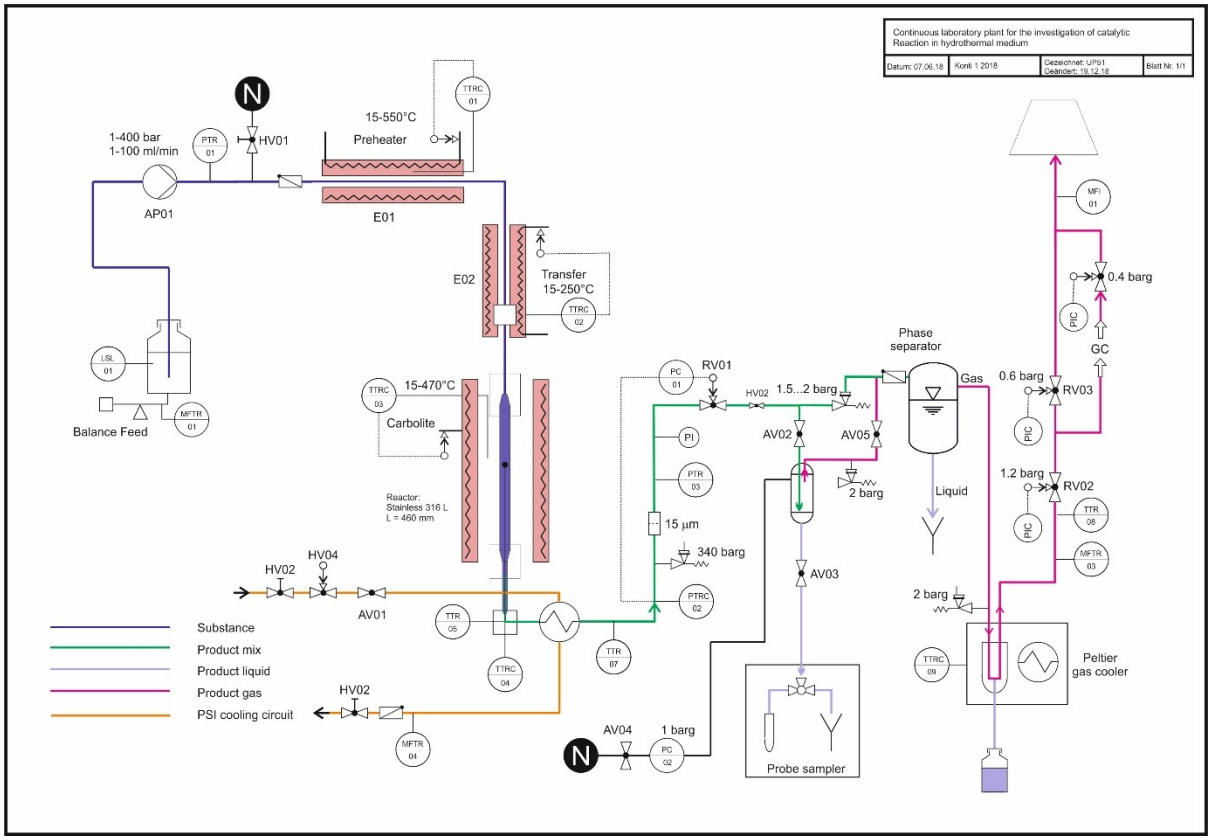

Fig. S0. P&ID of the continuous SCWG setup (Konti-I).

Gas generated during SCWG experiments was measured on-line using a µGC 3000 series (Inficon) equipped with two columns, i.e. Molsieve (10 m × 320 µm × 30 µm, for separation

of H_2, O_2, N_2, CH_4, and CO) and PLOTQ (8 m × 320 µm × 30 µm, for separation of CO_2, C_2H_4, C_2H_6, C_3H_6, and C_3H_8), as well as a thermal conductivity detector (TCD).

The carbon content of the process water was analysed on a Dimatoc2000 (DIMATEC) carbon analyser. The instrument determined the total carbon (TC) by oxidising the carbon into CO_2 at 850°C in a quartz reactor over a Pt/SiO_2 catalyst. The total inorganic carbon (TIC) was determined by converting the carbonates to CO_2 at 160°C by addition of H_3PO_4 (42.5 %) in a quartz vessel filled with porous silica gel beads. The total organic carbon (TOC) was calculated as the difference between TC and TIC (TOC = TC - TIC).

The carbon gasification efficiency GE_C was calculated as

$$GE_C\,[\%] = \frac{\dot{n}_{C,gas}}{\dot{n}_{C,feed}} \cdot 100\ \% \qquad (1)$$

where $\dot{n}_{C,gas}$ is the total carbon molar flow rate in the gas phase and $\dot{n}_{C,feed}$ is the carbon molar flow rate entering the reactor.

The carbon (glycerol) conversion was calculated as

$$X_C[\%] = \frac{\dot{n}_{TOC,feed} - \dot{n}_{TOC,out}}{\dot{n}_{TOC,feed}} \cdot 100\ \% \qquad (2)$$

where $\dot{n}_{TOC,feed}$ and $\dot{n}_{TOC,out}$, represent the total carbon molar flow rates of organic carbon entering and exiting the system, respectively.

The apparent carbon conversion rate calculated in two ways taking into account X_C or alternatively using GE_C,

$$r_{Xc}\left[\frac{g_C}{g_{Ru} \cdot h}\right] = \frac{\dot{m}_{C,feed} \cdot X_C}{100 \cdot m_{Ru,total}} \qquad (3)$$

$$r_{GEc}\left[\frac{g_C}{g_{Ru} \cdot h}\right] = \frac{\dot{m}_{C,feed} \cdot GE_C}{100 \cdot m_{Ru,total}} \qquad (4)$$

Mear's criterion was used to evaluate the external mass transfer and heat transfer limitations, which proved to be negligible. The influence of pore diffusion on reaction rate was estimated with the Weisz-Prater criterion, which indicated that pore diffusion limitations are negligible.

Mass Transfer Limitations: Internal Diffusion, Weisz–Prater Criterion (C_{WP})

The presence of internal mass transfer limitations was evaluated using the Weisz–Prater criterion. A C_{WP} value below 1 indicates that internal diffusion does not significantly affect the reaction, and thus, internal mass transfer limitations can be considered negligible.

$$C_{WP} = \frac{r_{obs} R_p^2}{C_S D_{eff}} \tag{5}$$

Where,

the reaction rate per volume of catalyst (r_{obs}) is $4.95 \cdot 10^{-2}$ mol·L_{cat}^{-1}·s^{-1} (maximum apparent carbon conversion rate);

the catalyst particle radius (R_p) is $8 \cdot 10^{-4}$ m (top of the size range);

the effective diffusivity (D_{eff}) is $1.281 \cdot 10^{-7}$ m^2·s^{-1};

the glycerol concentration at the surface of the particle is 0.3261 mol·L^{-1}.

$C_{WP} = 0.19 < 1$

Therefore, internal mass transfer limitations are not significant in this system.

Mass Transfer Limitations: External Diffusion, Mears' Criterion (C_M)

External mass transfer limitations were evaluated using the Mears' criterion. When C_M is less than 0.15, external mass transfer limitations are considered negligible, indicating that such limitations are not significant in the system studied.

$$C_M = \frac{r_{obs} \rho_b R_p n}{k_c C_{Ab}} \tag{6}$$

Where,

the observed reaction rate (r_{obs}) is $2.15 \cdot 10^{-5}$ mol·g_{cat}^{-1}·s^{-1};

the catalyst bed density (ρ_b) is 2300.00 kg·m^{-3};

the catalyst pellet radius (R_p) is $8 \cdot 10^{-4}$ m (top of the size range);

the reaction order of reactant glycerol (n) is 1;

the mass transfer coefficient of glycerol (k_c) is $7.54 \cdot 10^{-4}$ m·s^{-1};

the bulk gas concentration of glycerol (C_{Ab}) is 0.3261 mol·L^{-1}.

C_M =0.08 < 0.15

Therefore, this system is not affected by external mass transfer limitations.

Stability test in a batch reactor

The stability tests under SCWG or SCW conditions were performed using a batch reactor (BR) with a total volume of 28 mL (see details in [3]). Briefly, the solid sample (0.5 g) and glycerol feed or pure DI water (6.7 g) were added into the reactor tube, which was then tightly screwed using a torque wrench (120 Nm). The amount of solution was chosen to reach a pressure of 270 ± 5 bar at the targeted temperature. Then, the BR was immersed in a fluidised sand bath (IFB51, Techne) previously heated to 430°C, and after the desired reaction time the reaction was terminated by quickly immersing the BR in the vessel in a bath of room temperature water. After cooling down, the reactor was opened, and the solid sample was recovered by filtration. After drying at 110°C overnight, the sample was subjected to further analysis to determine its stability under the conditions applied.

Regeneration of spent Ru/CeO_2 catalysts

Regeneration of spent catalysts (remove of coke deposit) was carried out in flow conditions through hydrothermal oxidation with H_2O_2. Initially, the system pressure was increased to 250 bar and heated to 110 ± 5°C in a DI water flow (5 g·min^{-1}). Then, the water stream was replaced with a H_2O_2 (5 wt.% solution) and after 1 h it was switched to DI H_2O. The system was then heated to 385°C and cooled after 30 min. The regenerated catalyst was dried at 110°C overnight. The sample after the regeneration process was denoted as y%Ru/CeO_2_x_*R*, where *R* denotes the regenerated catalyst.

Bibliography

1. C. Hunston, D. Baudouin, L. Koning, A. Agarwal, O. Kröcher and F. Vogel, *Applied Catalysis B: Environmental*, 2023, 320, 121956
2. B. H. Toby and R. B. Von Dreele, *Journal of Applied Crystallography*, 2013, 46, 544–549
3. M. H. Waldner and F. Vogel, *Ind. Eng. Chem. Res.*, 2005, 44, 4543–4551.

Supporting figures

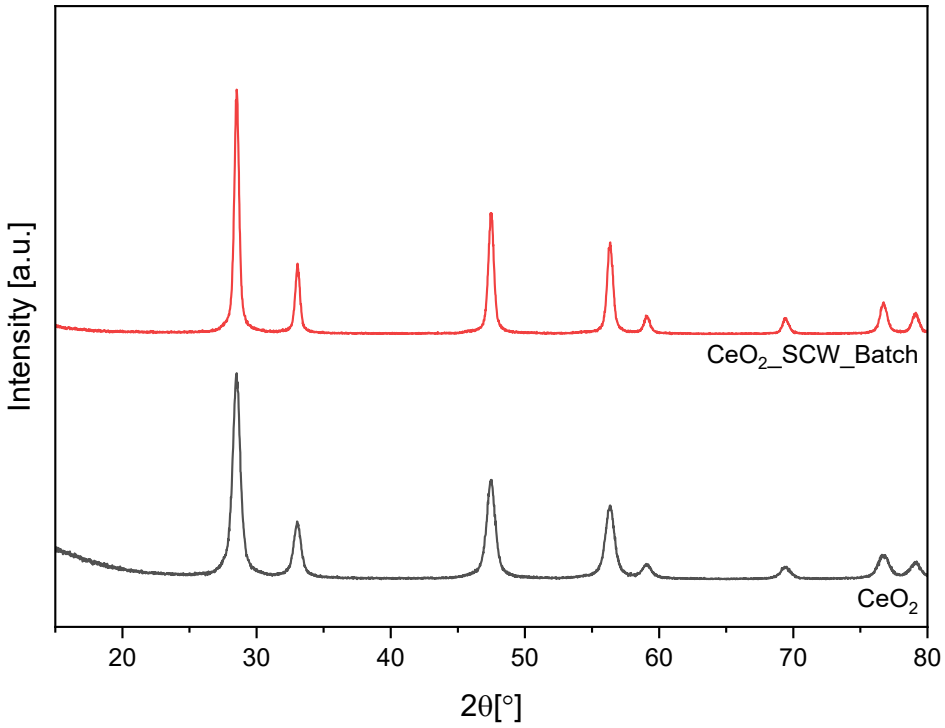

Fig. S1. XRD diffractograms of CeO_2 before and after the SCW test in a batch reactor.

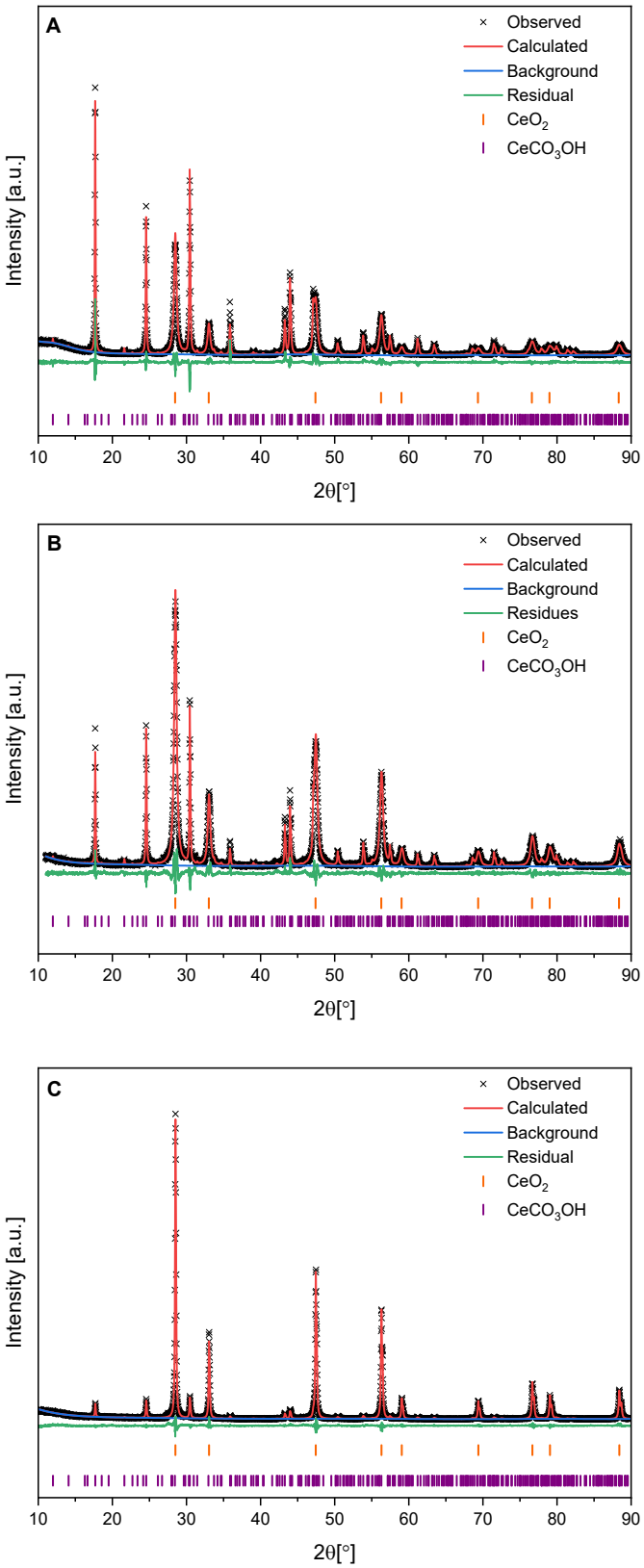

Fig. S2. XRD patterns and Rietveld refinement for CeO_2 after the SCWG (A), CeO_2 after the SCWG with pH control (B) and CeO_2_900 after the SCWG. The observed, calculated, background and difference are shown.

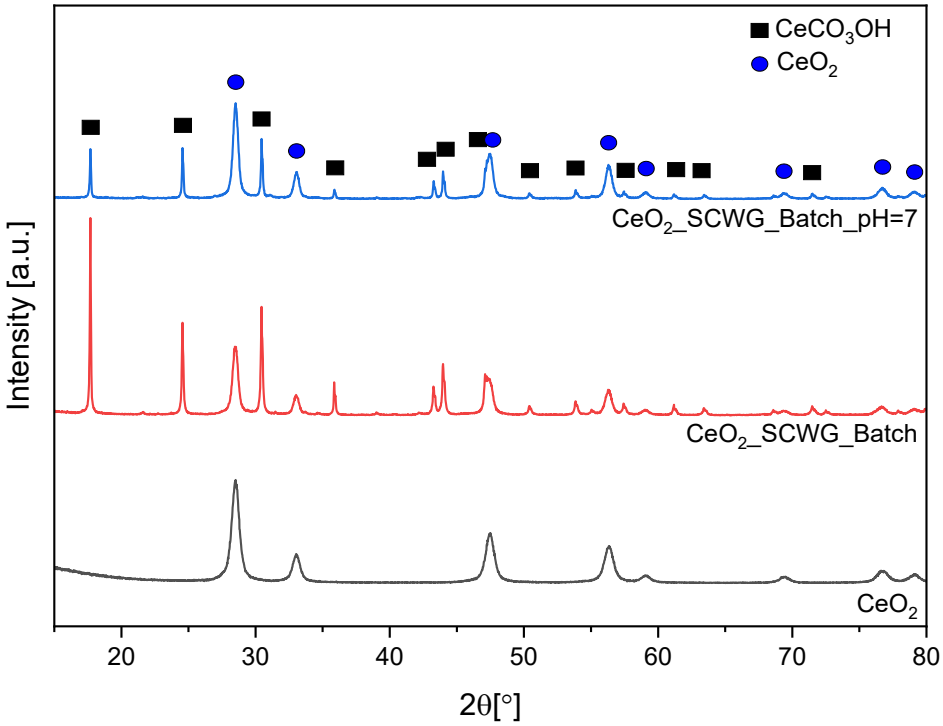

Fig. S3. XRD patterns of CeO_2 before and after the SCWG test in batch reactor with and without pH control.

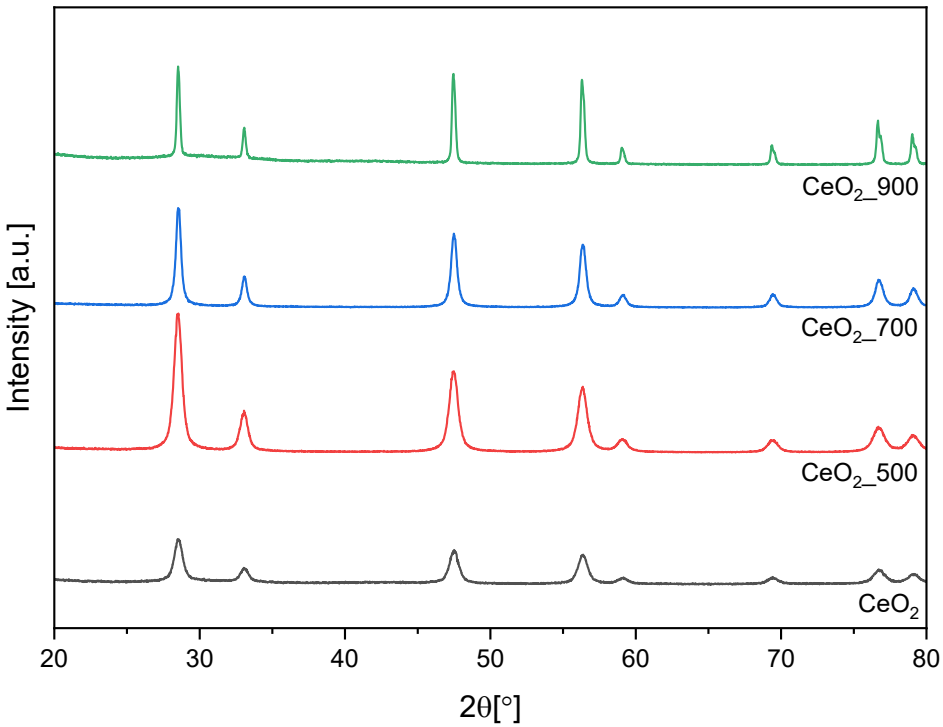

Fig. S4. XRD patterns of the CeO_2 before and after calcination at different temperatures.

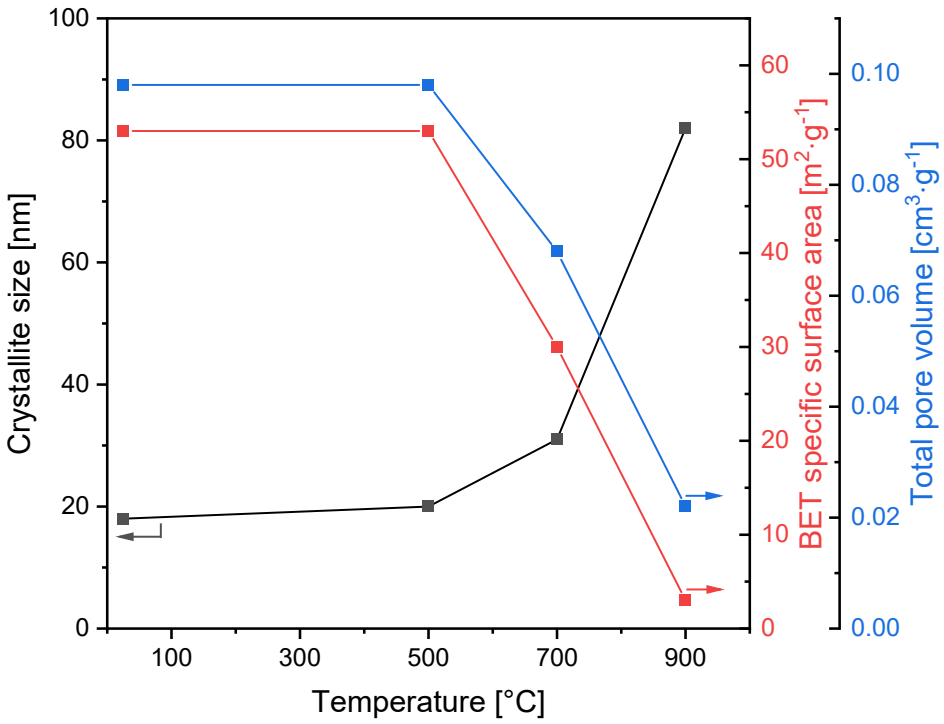

Fig. S5. Dependence between crystallinity, BET specific surface area, total pore volume and calcination temperature.

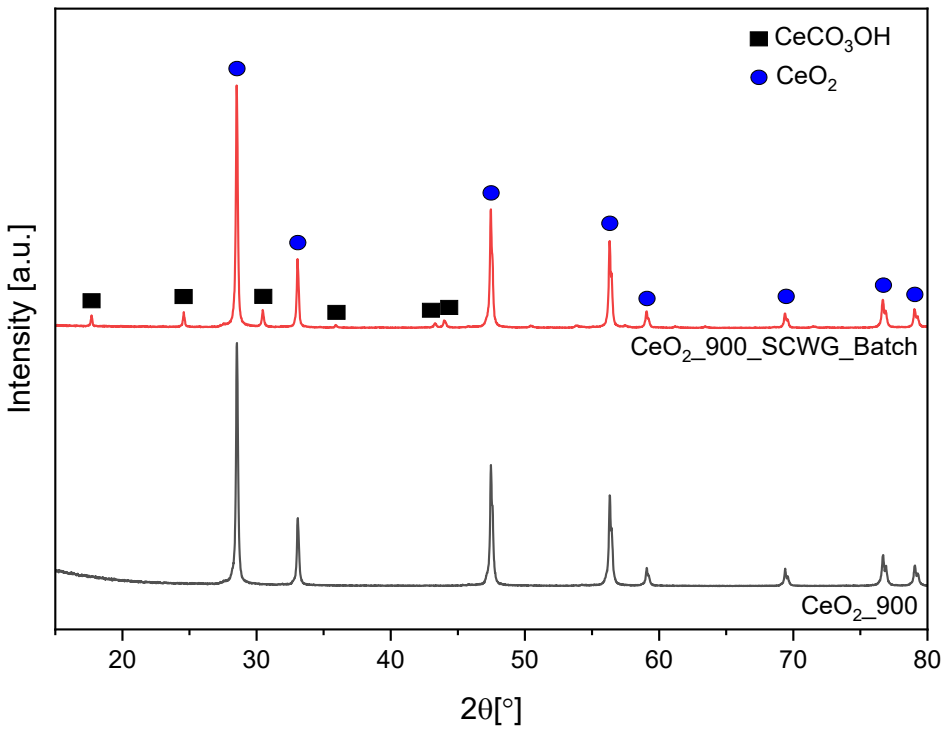

Fig. S6. XRD diffractograms of CeO_2_900 before and after the SCWG test in a batch reactor.

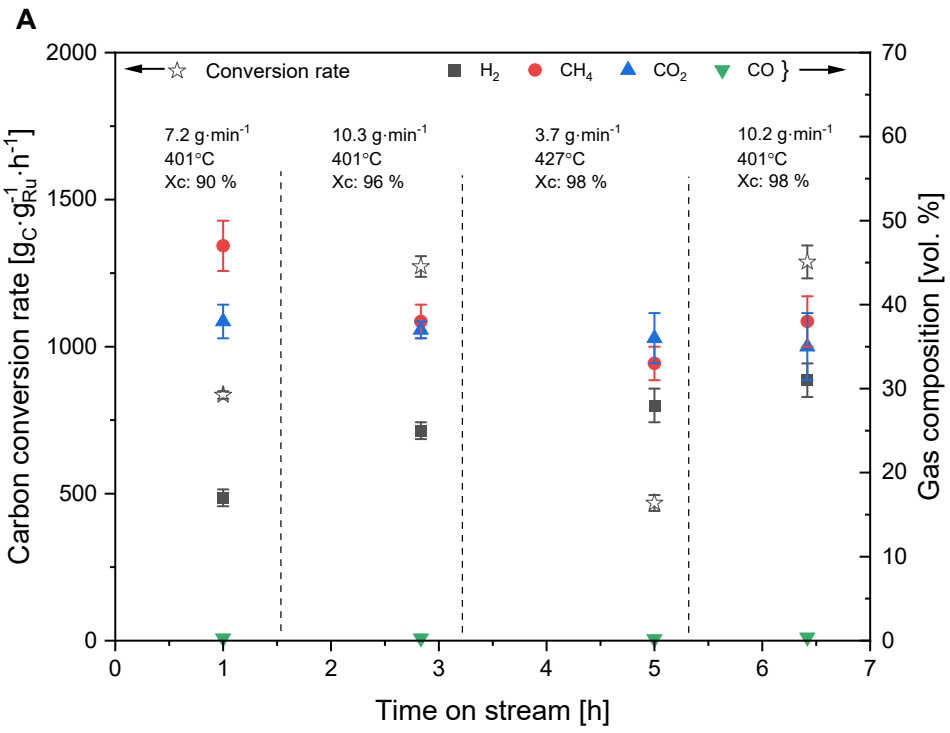
A
Conversion rate
H2
CH4
CO2
CO
7.2 g·min-1
401°C
Xc: 90 %
10.3 g·min-1
401°C
Xc: 96 %
3.7 g·min-1
427°C
Xc: 98 %
10.2 g·min-1
401°C
Xc: 98 %
Carbon conversion rate [gC·gRu-1·h-1]
Gas composition [vol. %]
Time on stream [h]

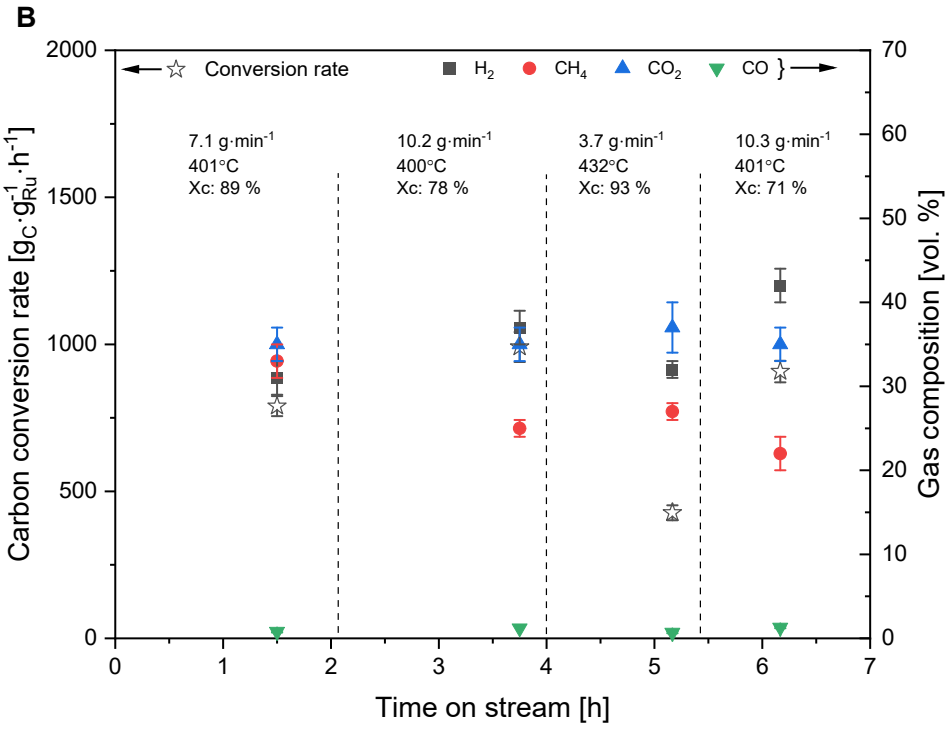
B
Conversion rate
H2
CH4
CO2
CO
7.1 g·min-1
401°C
Xc: 89 %
10.2 g·min-1
400°C
Xc: 78 %
3.7 g·min-1
432°C
Xc: 93 %
10.3 g·min-1
401°C
Xc: 71 %
Carbon conversion rate [gC·gRu-1·h-1]
Gas composition [vol. %]
Time on stream [h]

C

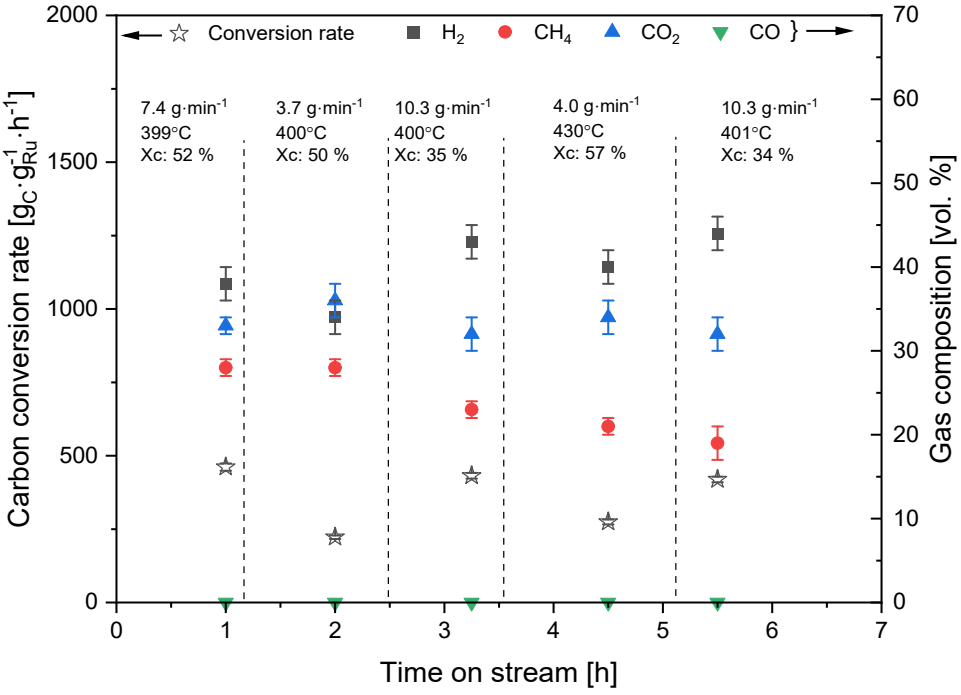
Conversion rate
H2
CH4
CO2
CO
7.4 g·min-1
399°C
Xc: 52 %
3.7 g·min-1
400°C
Xc: 50 %
10.3 g·min-1
400°C
Xc: 35 %
4.0 g·min-1
430°C
Xc: 57 %
10.3 g·min-1
401°C
Xc: 34 %
Carbon conversion rate [gC·gRu-1·h-1]
Gas composition [vol. %]
Time on stream [h]

D

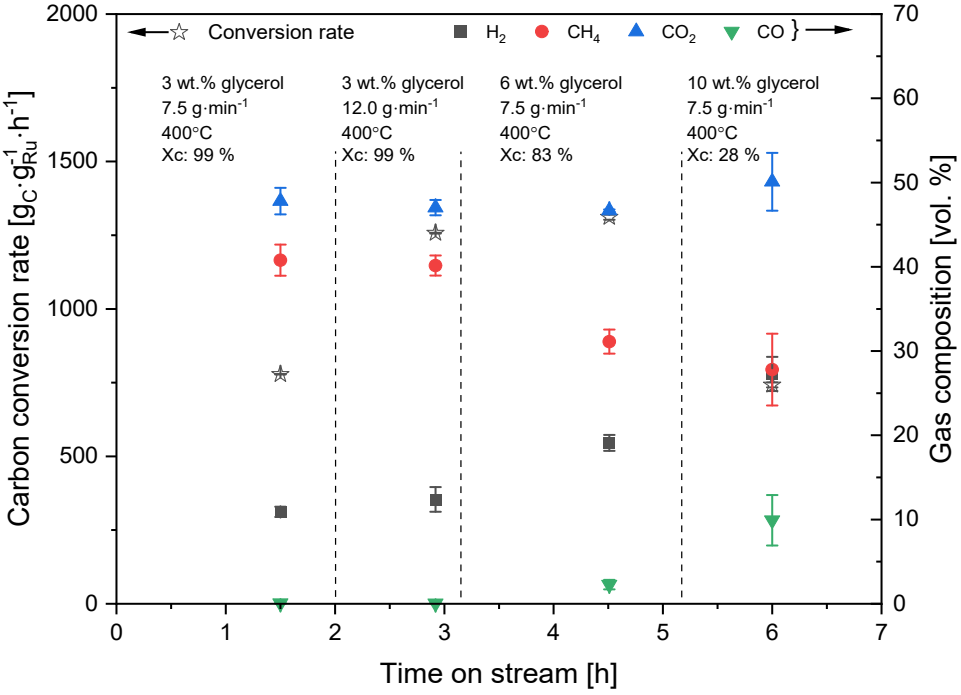
Conversion rate
H2
CH4
CO2
CO
3 wt.% glycerol
7.5 g·min-1
400°C
Xc: 99 %
3 wt.% glycerol
12.0 g·min-1
400°C
Xc: 99 %
6 wt.% glycerol
7.5 g·min-1
400°C
Xc: 83 %
10 wt.% glycerol
7.5 g·min-1
400°C
Xc: 28 %
Carbon conversion rate [gC·gRu-1·h-1]
Gas composition [vol. %]
Time on stream [h]

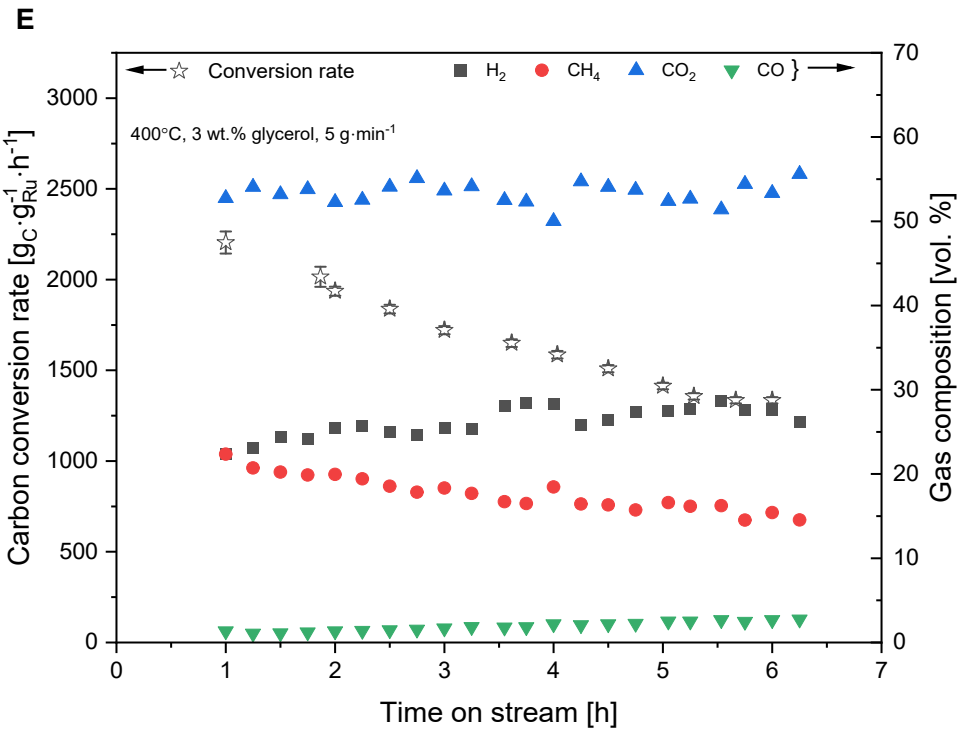

Fig. S7. Apparent carbon conversion rate and gas composition for 0.11%Ru/CeO_2_900 (A), 0.25%Ru/CeO_2_700 (B), 1.00%Ru/CeO_2_700 (C), 0.44%Ru/CeO_2_700 (D and E). SCWG conditions given in the Figures.

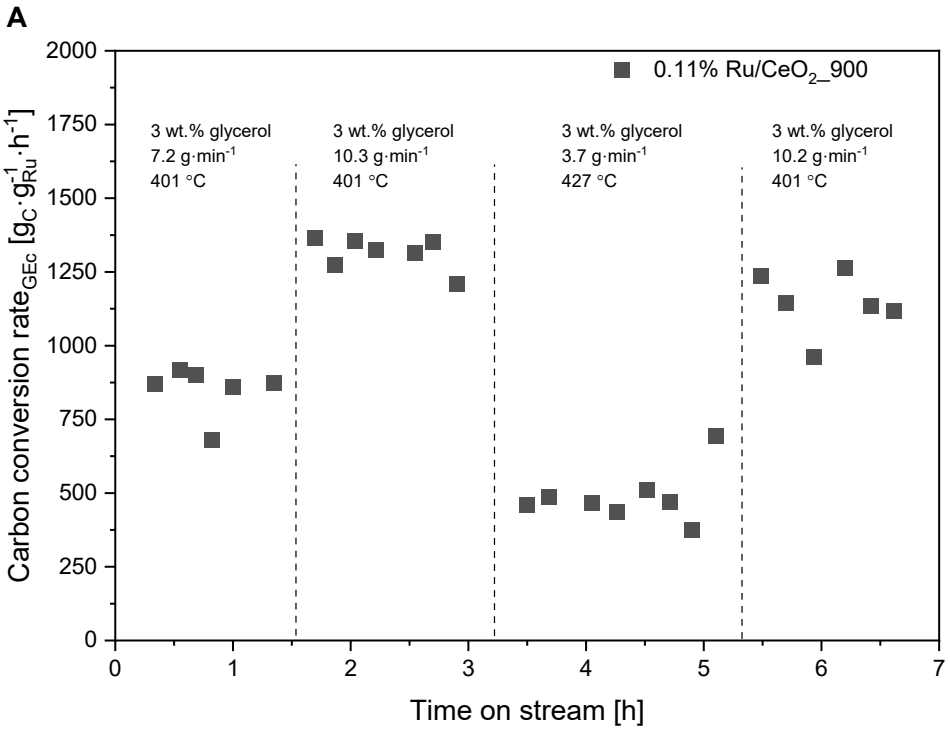
A
0.11% Ru/CeO2_900
3 wt.% glycerol
7.2 g·min-1
401 °C
3 wt.% glycerol
10.3 g·min-1
401 °C
3 wt.% glycerol
3.7 g·min-1
427 °C
3 wt.% glycerol
10.2 g·min-1
401 °C
Carbon conversion rateGEc [gC·gRu-1·h-1]
Time on stream [h]

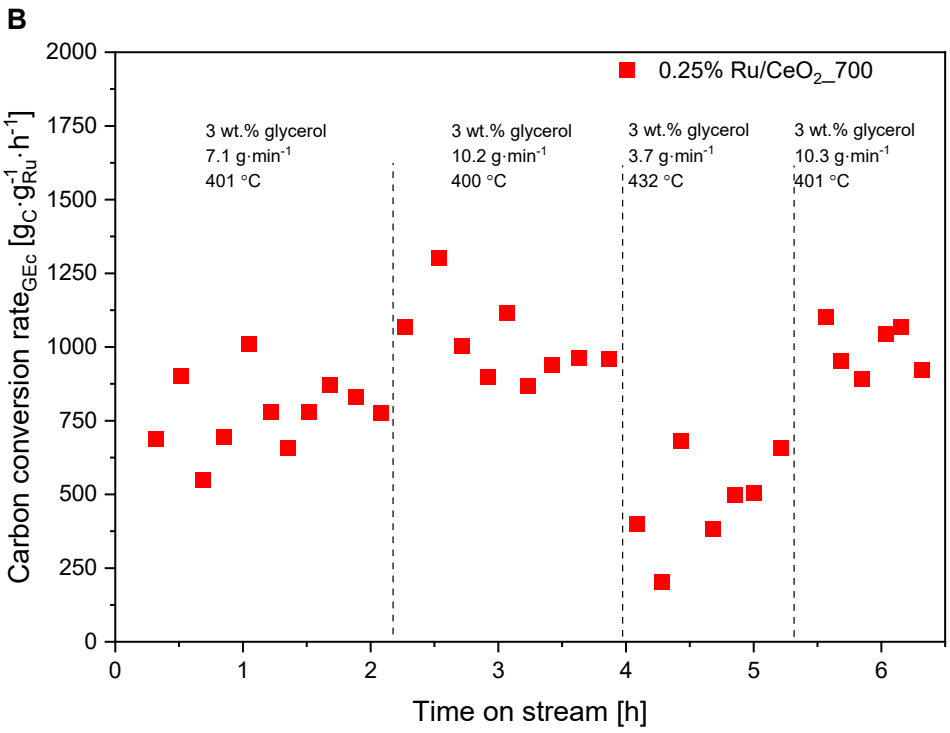
B
0.25% Ru/CeO2_700
3 wt.% glycerol
7.1 g·min-1
401 °C
3 wt.% glycerol
10.2 g·min-1
400 °C
3 wt.% glycerol
3.7 g·min-1
432 °C
3 wt.% glycerol
10.3 g·min-1
401 °C
Carbon conversion rateGEc [gC·gRu-1·h-1]
Time on stream [h]

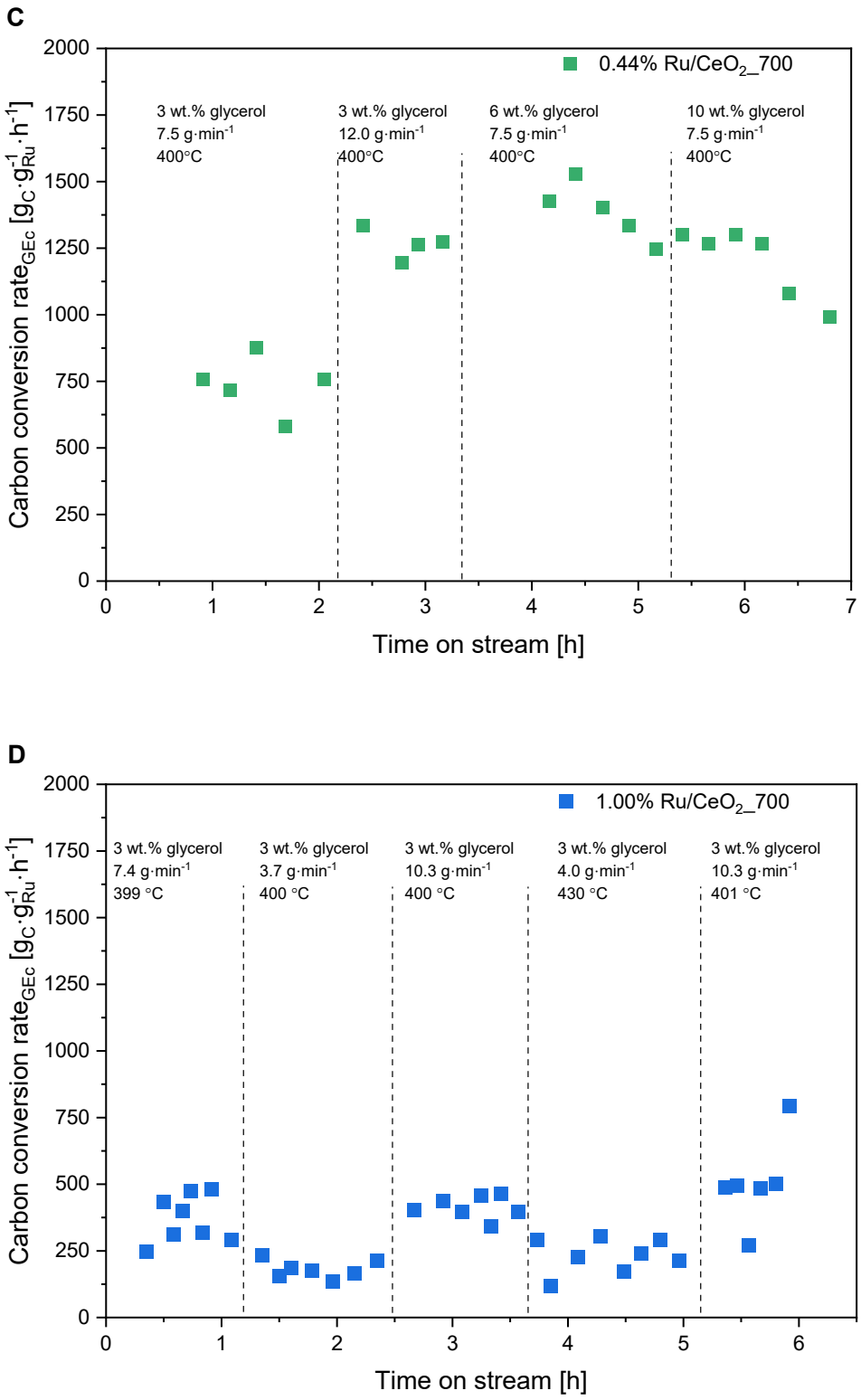

Fig. S8. Apparent carbon conversion rate based on gas efficiency values for 0.11%Ru/CeO_2_900 (A), 0.25%Ru/CeO_2_700 (B), 0.44%Ru/CeO_2_700 (C) and 1.00%Ru/CeO_2_700 (D). SCWG conditions given in the Figures.

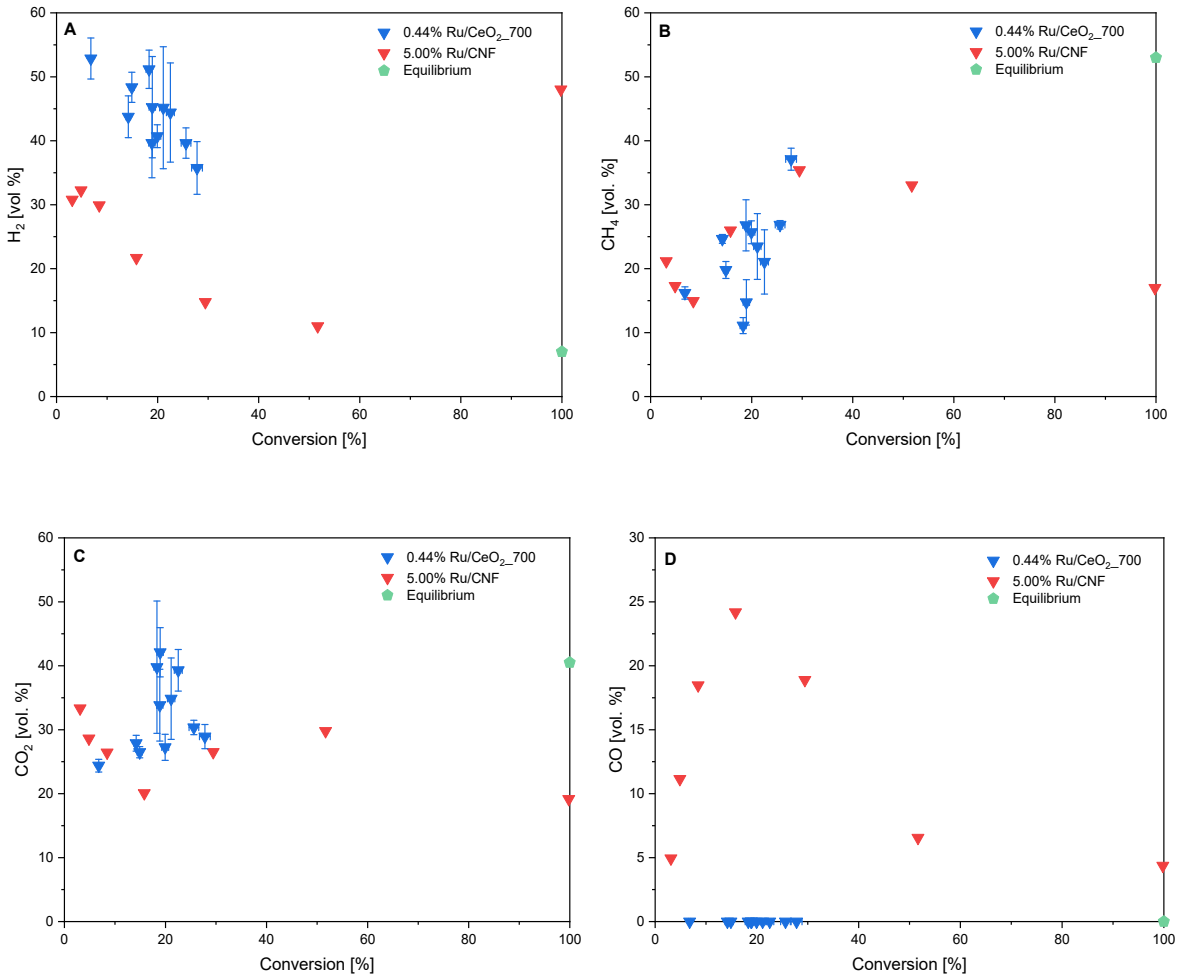

Fig. S9. Dependence between gas composition and conversion of glycerol (10 wt.%) achieved at 400°C and 270 bar over 0.44%Ru/CeO_2_700 and 5.00%Ru/CNF catalysts.

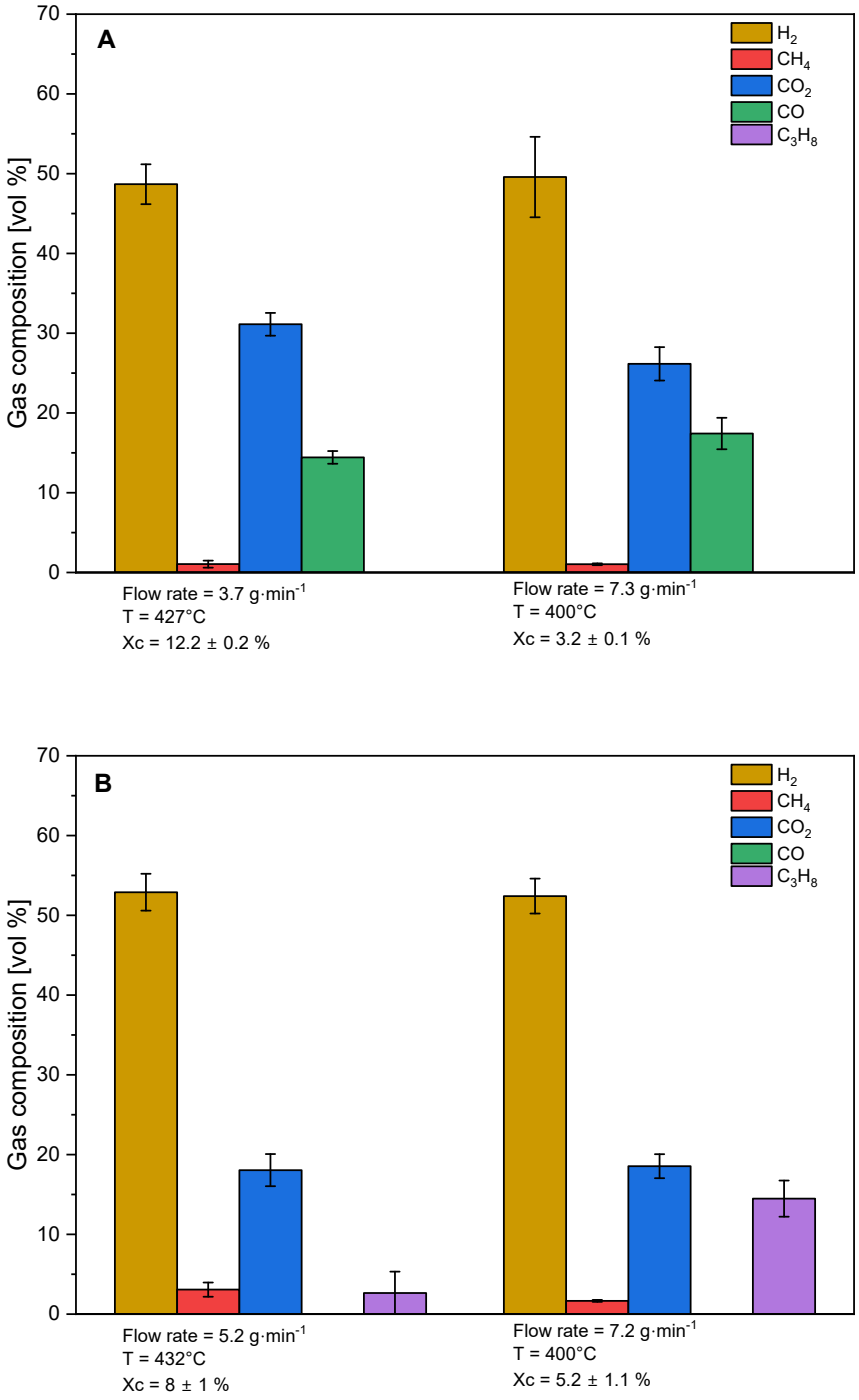

Fig. S10. Comparison of gas composition achieved during SCWG over CeO_2 calcined at 700°C (A) and after subsequent reduction in H_2 (B).

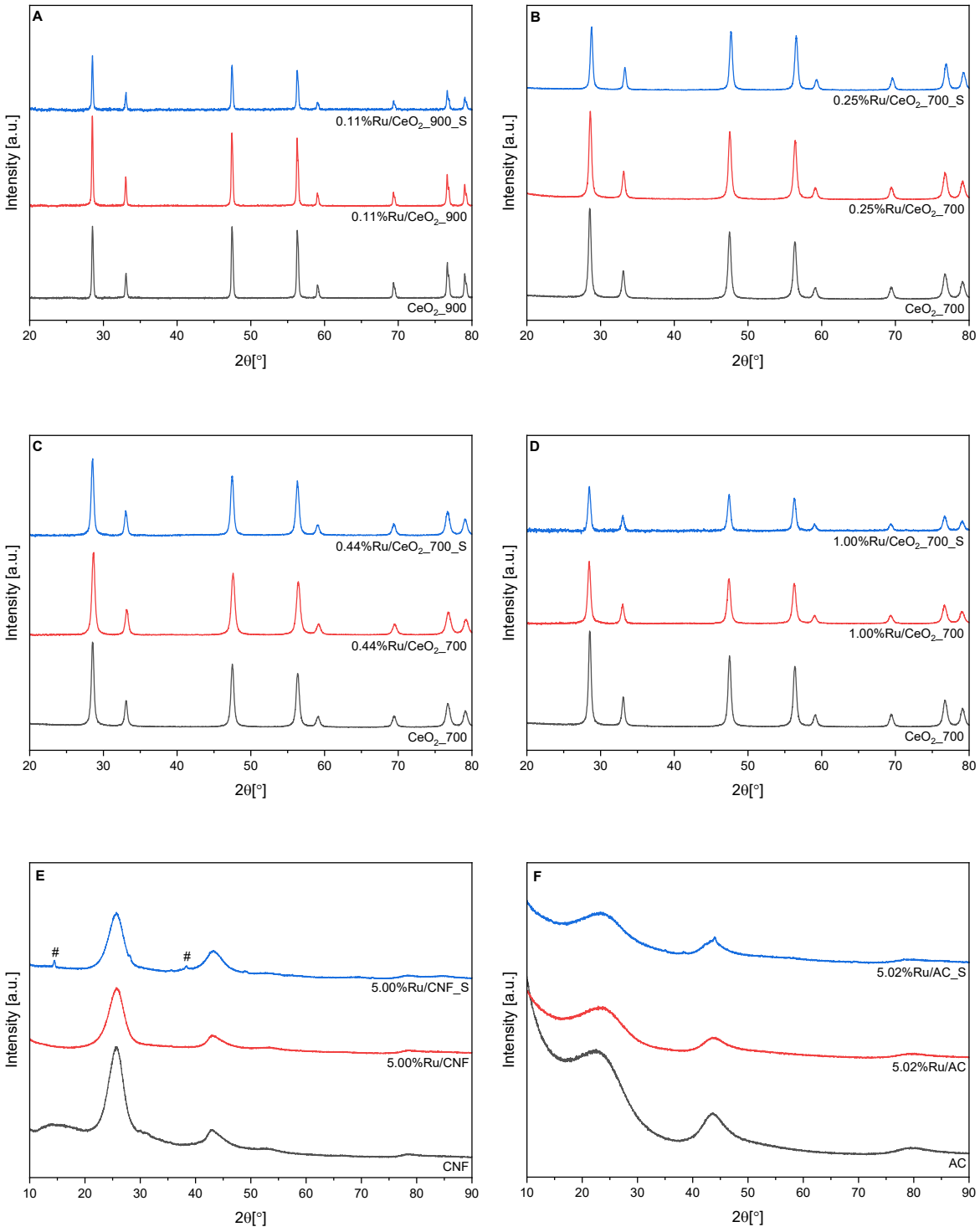

Fig. S11. XRD patterns for supports and fresh as well as spent Ru/CeO_2 (A-D), Ru/CNF (E) and Ru/AC (F) catalysts. The symbol # indicates contamination from a component of the high-temperature paste used on the reactor threads.

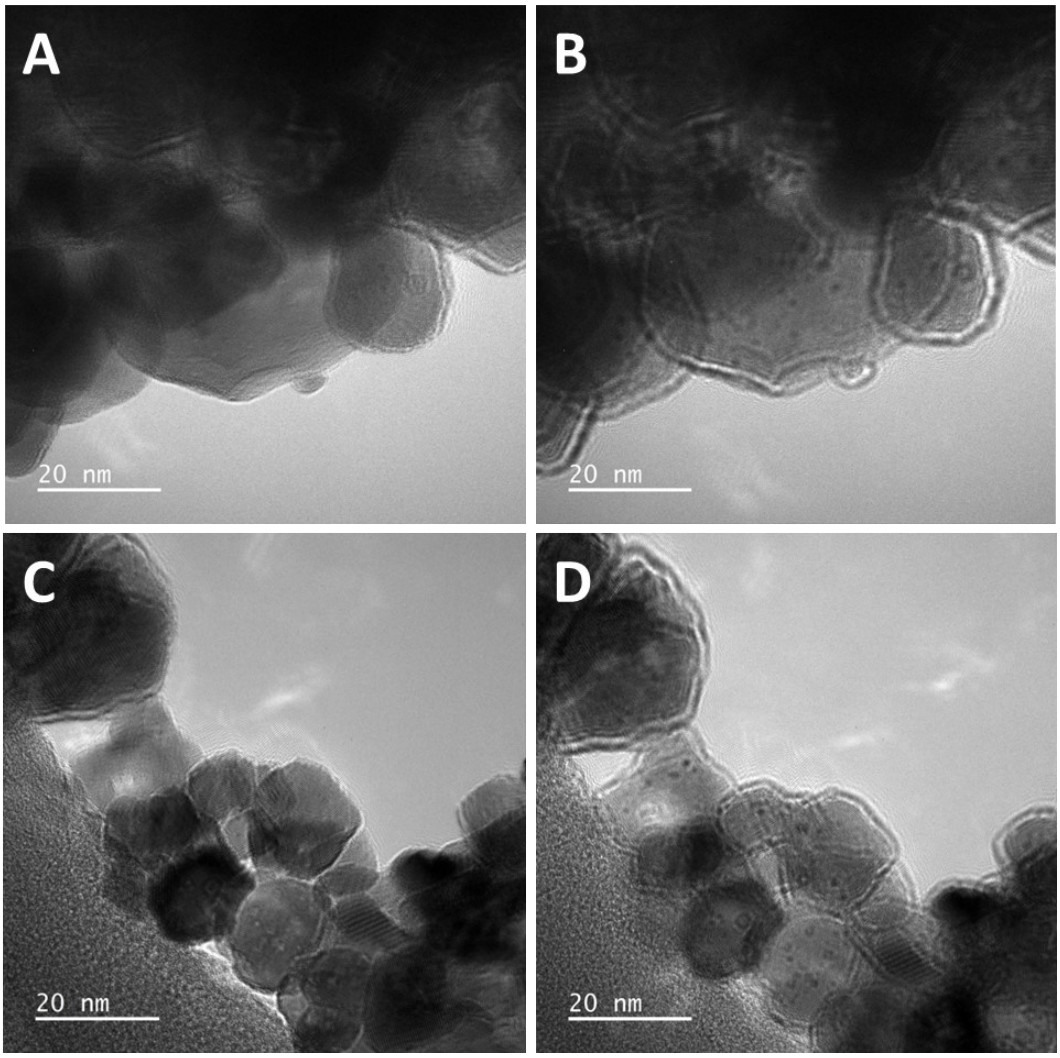

Fig. S12. HR-TEM images of the CeO_2_700 (A, B) and 0.44%Ru/CeO_2_700 (C, D); the same spots taken with a different focus.

Note that, the occurrence of these darker spots (potential Ru nanoparticles) is highly dependent on the appropriate focusing during the TEM measurement.

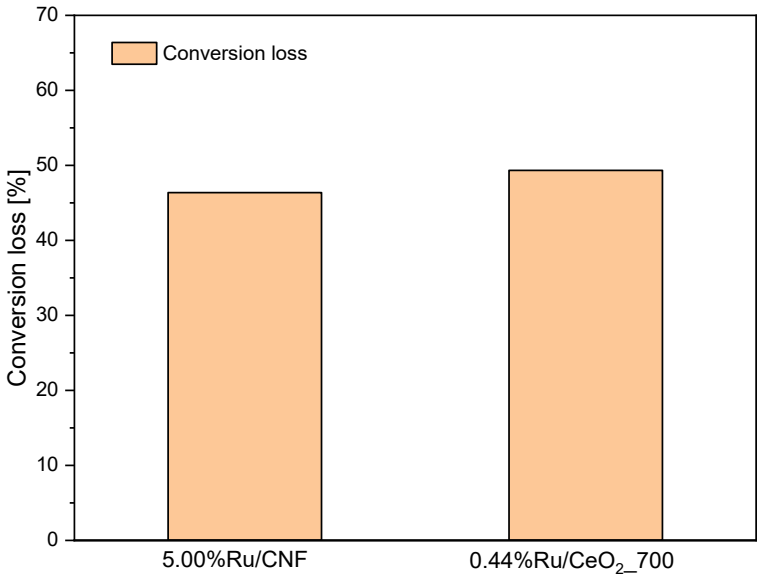

Fig. S13. Expected glycerol conversion loss after hundreds of hours on stream SCWG of 3wt.% glycerol at 400°C.

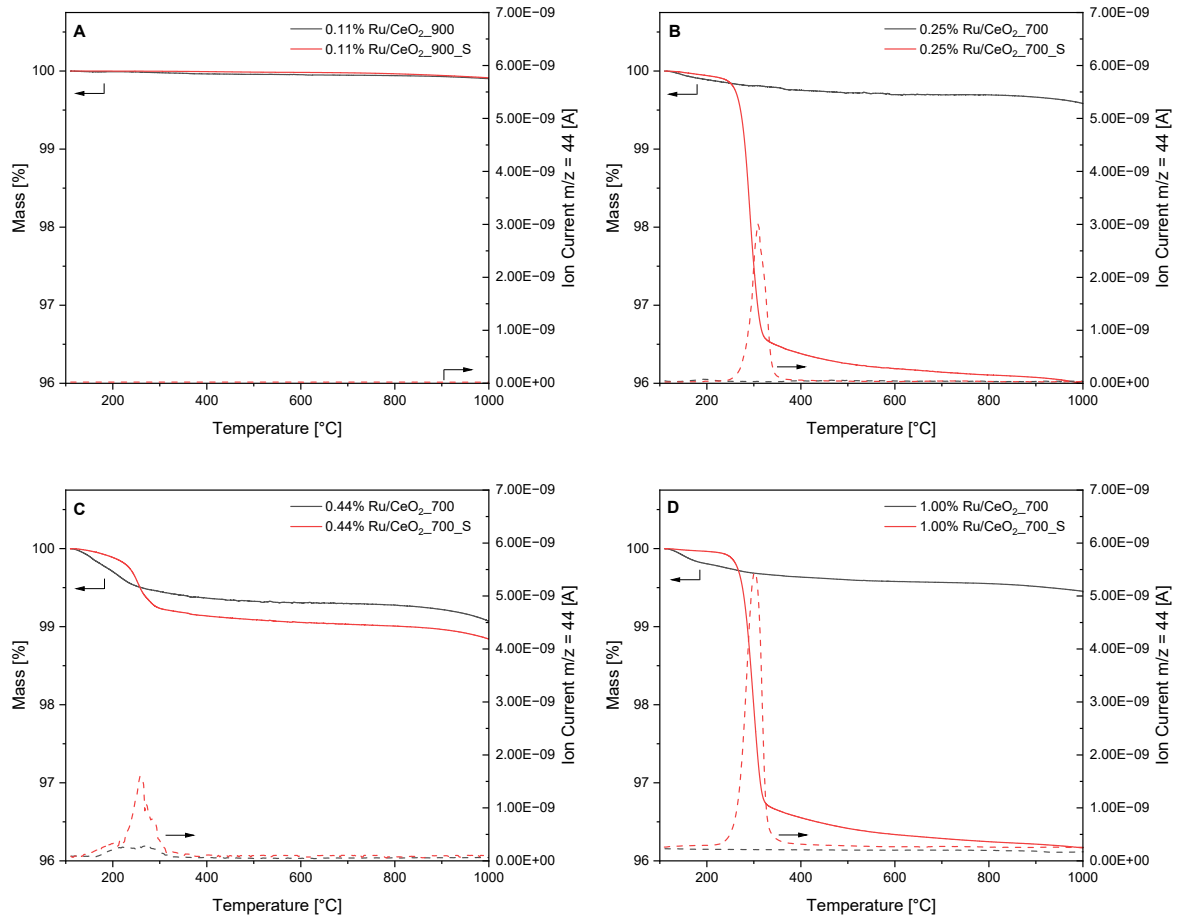

Fig. S14. TGA profiles (solid line) and m/z = 44 MS line assigned to CO_2 released during heating ramp (dashed line) for fresh (black) and spend (red) catalysts; 0.11%Ru/CeO_2_900 (A), 0.25%Ru/CeO_2_700 (B), 0.44%Ru/CeO_2_700 (C) and 1.00%Ru/CeO_2_700 (D).

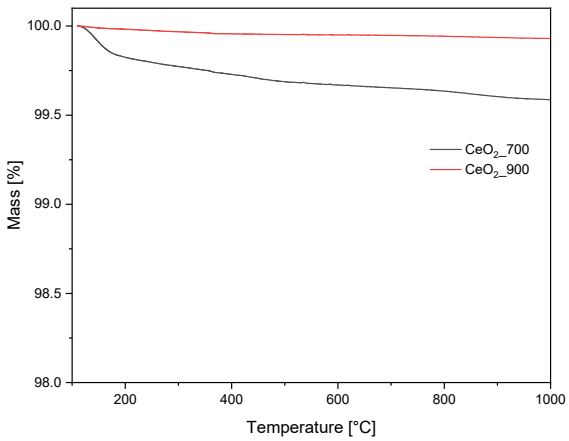

Fig. S15. TGA profiles of CeO_2_700 and CeO_2_900 support.

Supporting tables

Table S1. Selected crystallographic data of the CeO_2 sample after various treatments.

Sample	CeO_2		$CeCO_3OH$		
	***a=b=c* lattice parameters [Å]**	**crystallite size [nm]**	***a=b* lattice parameters [Å]**	***c* lattice parameter [Å]**	**crystallite size [nm]**
CeO_2_SCWG_Batch	5.413	30	12.519	9.991	304
CeO_2_SCWG_Batch_pH=7	5.412	28	12.519	9.992	180
CeO_2_900_SCWG_Batch	5.410	93	12.523	9.992	134

Table S2. Crystal properties of the CeO_2 samples.

Sample	Lattice parameter[1] ***a*** **[Å]**	Crystallite size[1] [nm]
CeO_2	5.410	18
CeO_2_500	5.411	20
CeO_2_700	5.411	31
CeO_2_900	5.412	82

[1] *Lattice parameter a and crystallite size of CeO_2 evaluated via Rietveld refinement.*

Table S3. Textural properties of the CeO_2 samples before and after SCWG test.

Sample	S_{BET} [$m^2 \cdot g^{-1}$]	ΔS_{BET} [%]	V_{total} [$cm^3 \cdot g^{-1}$]	ΔV_{total} [%]
CeO_2	53	N/A	0.098	N/A
CeO_2_SCWG_Batch	7.0	- 87	0.028	- 71
CeO_2_SCWG_Continuous	20	- 62	0.095	- 3
CeO_2_700	30	N/A	0.068	N/A
CeO_2_700_SCWG_Continuous	18	- 40	0.067	- 1
CeO_2_900	3.0	N/A	0.022	N/A
CeO_2_900_SCWG_Batch	3.0	0	0.022	0
CeO_2_900_SCWG_Continuous	2.9	-3	0.022	0

Table S4. Evolution of particle size obtained from TEM, calculated from the specific surface area assuming a density of 7.2 g·cm^{-3} and spherical particles, and CeO_2 crystallite size calculated from the Scherrer equation and via Rietveld refinement in Ru/CeO_2 catalysts before and after continuous SCWG of glycerol.

Sample	Particle size[1] [nm]	d_{BET}[2] [nm]	Crystallite size[3] [nm]	Crystallite size[4] [nm]
CeO_2_900	n.d.	280	38 ± 1	82
0.11%Ru/CeO_2_900	41 ± 12	280	41 ± 4	91
0.11%Ru/CeO_2_900_S	45 ± 13	290	41 ± 5	94
CeO_2_700	n.d.	28	20 ± 1	31
CeO_2_700_S	n.d.	46	22 ± 1	29
0.25%Ru/CeO_2_700	17 ± 4	29	22 ± 1	30
0.25%Ru/CeO_2_700_S	22 ± 6	75	22 ± 1	36
0.25%Ru/CeO_2_700_SCW[5]	22 ± 4	52	24 ± 2	34
0.44%Ru/CeO_2_700	16 ± 3	24	18 ± 1	26
0.44%Ru/CeO_2_700_S	23 ± 6	49	20 ± 1	30
1.00%Ru/CeO_2_700	16 ± 3	27	18 ± 1	26
1.00%Ru/CeO_2_700_S	23 ± 6	69	21 ± 1	26

[1] Particle size of CeO_2 based on TEM observation.

[2] Calculated from the specific surface area assuming a density of 7.2 g·cm^{-3} and spherical particles.

[3] Crystallite size of CeO_2 calculated according to Scherrer equation: $D_{(hkl)}=0.9\cdot\lambda/(\beta\cdot\cos\vartheta)$, $\lambda=0.154$ nm, ϑ is the Bragg diffraction angle (deg.), and β is the FWHM (rad.) of the diffraction peaks. Average based on (111), (220) and (311).

[4] Crystallite size of CeO_2 evaluated via Rietveld refinement.

[5] Test performed in batch experiment with pure water for 1 hour at 270 bar, 430°C, to mimic the conditions the catalyst is exposed before the start of a continuous test.

Table S5. Size of identified particles (which can be assigned to both Ru- and CeO_2-based species) in the Ru/CeO_2 samples before and after SCWG experiment. Ru/CNF was used as reference.

Catalyst	**Particle size [nm]**	
	Fresh	**Spent**
0.11%Ru/CeO_2_900	1.3 ± 0.3	2.1 ± 0.6
0.25%Ru/CeO_2_700	1.6 ± 0.4	2.3 ± 0.7
0.44%Ru/CeO_2_700	1.2 ± 0.2	1.8 ± 0.5
1.00%Ru/CeO_2_700	1.0 ± 0.2	2.5 ± 0.5
5.00Ru/CNF	2.0 ± 0.6[1]	3.1 ± 0.8[1]

[1] Ru particle size comparable to that reported in previous studies [1].

[1] C. Hunston, D. Baudouin, L. Koning, A. Agarwal, O. Kröcher and F. Vogel, Applied Catalysis B: Environmental, 2023, 320, 121956